



# Influence of Ambient Conditions on the Qualification Tests of the Interturn Insulation in Low-Voltage Electrical Machines

Niklas Driendl , Florian Pauli , and Kay Hameyer, *Senior Member, IEEE*

**Abstract**—An increased dc-link voltage and fast-switching semiconductors constitute new challenges on the insulation system of low-voltage electrical machines, especially in automotive applications. During the design process, the different components of the insulation system can be tested according to IEC 60034-18-41. This industrial standard prescribes certain test voltages for type-I insulation systems based on empirical values. However, important ambient influence factors such as humidity and air pressure are not considered. Therefore, this work focuses on the influence of ambient conditions on the insulation strength of low-voltage electrical machines. Partial discharge tests are performed on specimens representing the interturn insulation which is usually regarded to be the weakest part of the insulation system. To represent the electrical stress during inverter operation, a bipolar test voltage is applied. The results of the measurements show that the standard is not applicable for the studied conditions in this work. It is concluded that the humidity and especially the ambient pressure have to be considered. The standard method using safety factors to calculate the test voltage is discussed. The method is extended to consider ambient conditions which are not covered by the standard.

**Index Terms**—Electrical machine, insulation system, interturn insulation.

## I. INTRODUCTION

TO achieve a faster battery charging process of electric vehicles, the dc-link voltage can be increased. In automotive industry, the commonly used 400 V-systems are expected to be replaced by 800 V-systems, which means that the electrical stress on the insulation components increases. As a benefit, the increase of the voltage leads to lower losses and weight savings due to lighter cables [1]. Additionally, the utilization of fast-switching semiconductors (e.g., SiC or GaN) moves into focus, providing a higher possible switching frequency and lower

switching losses [2]. However, the low voltage rise time  $t_r$  and high slope  $du/dt$  cause higher overvoltages when compared to conventionally used silicon-based semiconductors with a lower voltage rise time and increased risk of partial discharge (PD) inception [3]–[6]. Partial discharges occur inside air inclusions between adjacent wires or between a wire and the stator core, as pictured in Fig. 1. Usually, the winding insulation (turn-to-turn) is considered to be the weakest part of the insulation system [7]. According to IEC 60034-18-41 [8], the insulation system of a low-voltage electrical machine rated below an effective voltage of 700 V is classified as a type-I system which must be partial discharge free for the entire lifetime. This value refers to the phase-to-phase rms value.

The different components of the insulation system are tested by applying a certain test voltage which the components must withstand without the inception of a partial discharge. According to [8], the lowest voltage at which a partial discharge occurs is defined as the partial discharge inception voltage (PDIV). During a test procedure, where the PDIV is exceeded, partial discharges occur frequently. When the applied voltage is continuously decreased, partial discharges extinguish when the partial discharge extinction voltage (PDEV) is reached.

The test voltage for qualification tests depends on different enhancement factors taking into account that the insulation capability is lowered by, e.g., the influence of a high temperature. Other ambient influences such as humidity and air pressure are not considered in this standard. Based on the physics about partial discharge processes, it is obvious that these factors affect the discharge phenomena and therefore the PDIV and PDEV. Especially in the field of more electric aircraft (MEA), the insulation strength has to be evaluated for high altitudes. Therefore, several studies are performed to evaluate the influence of air pressure [9]–[11]. The standard distinguishes between qualification tests and type tests. For type tests, an aging process is considered by applying an additional enhancement factor. The influence of ambient conditions on the partial discharge resistance is studied in several publications [12]–[15], but a methodology to improve the current standard has not been developed yet.

It can be stated that the design based on empirically defined enhancement factors can lead to an inappropriate dimensioning of the insulation system [7]. A more precise dimensioning can be achieved with an individual material examination. Additionally, it has to be investigated how the influence factors correlate to each other to ensure the applicability of the provided method.

Manuscript received January 25, 2021; revised April 30, 2021 and July 27, 2021; accepted August 19, 2021. Date of publication September 3, 2021; date of current version March 1, 2022. (Corresponding author: Niklas Driendl.)

The authors are with the Institute of Electrical Machines, RWTH Aachen University, 52062 Aachen, Germany (e-mail: niklas.driendl@iem.rwth-aachen.de; florian.pauli@iem.rwth-aachen.de; hameyer@iem.rwth-aachen.de).

Color versions of one or more figures in this article are available at <https://doi.org/10.1109/TIE.2021.3108721>.

Digital Object Identifier 10.1109/TIE.2021.3108721

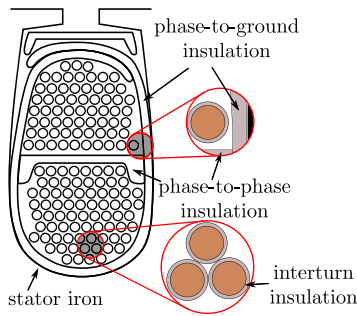


Fig. 1. Cross section of an exemplary stator slot.

This article therefore focusses to use the method given by IEC 60034-18-41 to calculate the test voltage and extend the standard to consider operating conditions which are not yet covered. Moreover, the mechanisms of partial discharge processes influenced by temperature, pressure and humidity are discussed in this work.

This article is organized as follows. In Section II, the mechanics of partial discharge processes are discussed. Section III gives an overview of the method to calculate the test voltage for type-I insulation systems given by the standard. In Section IV, the measurement setup is introduced. In the following section, the measurement results of the PDIV and PDEV are presented for the different ambient influences. The experiments are carried out on twisted pairs. The results are used in Section VI to compensate the operation conditions, which are not considered by the standard.

## II. PARTIAL DISCHARGE PROCESSES

In this section, mechanisms of partial discharge are discussed including the role of charge carrier accumulation and the influence of ambient conditions.

### A. Charge Carrier Accumulation

Partial discharge processes are initiated by a starting electron colliding with a gas molecule. In addition to a starting electron, a sufficiently high electric field strength is required. Through this process, electrons are released from the molecule and move toward the anode. The residual positive ions move in the direction of the cathode. The free charge carriers accumulate at the insulation surfaces creating an electric field  $E_{sc}$  with an opposite direction to the external field  $E_{ext}$ . In inverter-driven electrical machines, polarity changes of the pulsed voltage occur. An exemplary course of the voltage and the corresponding charge carrier accumulations are shown in Fig. 2. After the first partial discharge occurs, the total electric field between two wires is weakened by the electric field created by the accumulated charge carriers at the insulation surfaces. When the polarity of the external voltage  $U$  changes, the magnitude of the total electric field is increased by the electric field component  $E_{sc}$  again leading to a partial discharge. Due to this mechanism, partial discharges occur continuously. The partial discharges disappear only when the external voltage is decreased so that the magnitude of the total electric field is below the critical voltage.

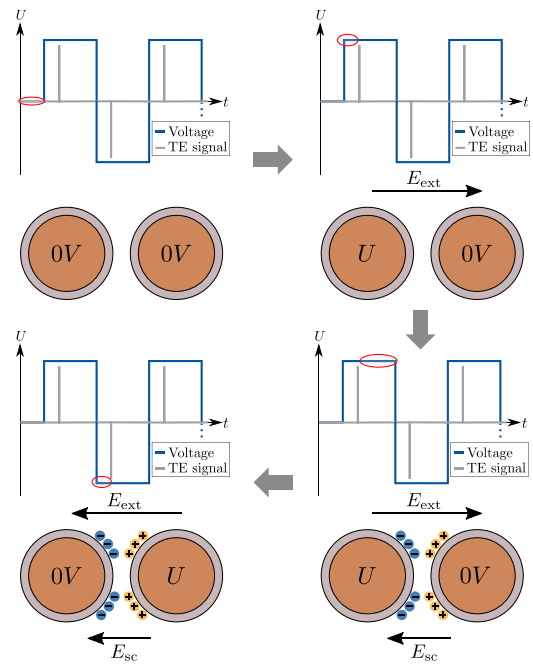


Fig. 2. Charge carrier accumulation.

### B. Effect of Ambient Conditions on PD Mechanisms

The influence of air pressure on the PDIV can be explained considering the *Townsend* equation. A variant of this equation is shown as follows:

$$E_{bd} = \frac{B \cdot p}{\ln(A \cdot p \cdot d) - \ln\left(1 - \frac{1}{\gamma}\right)}. \quad (1)$$

In this equation,  $E_{bd}$  is the breakdown electric field strength depending on the specific gas parameters  $A$  and  $B$ , the distance  $d$  and the secondary-electron-emission coefficient  $\gamma$ . Typical values for the parameters  $A$  and  $B$  are  $10.951/(\text{Pa} \cdot \text{m})$  and  $273.8 \text{ V}/(\text{Pa} \cdot \text{m})$  considering a discharge process in air. The parameter  $\gamma$  indicates the number of electrons released by the impact of positive ions on the cathode. The value depends on the combination of cathode material and gas and is well known for metallic cathode materials. As an example, the value for the combination of air and iron is 0.02. For polymeric materials, the value is assumed to be significantly lower because of the higher work function. This equation shows the general influence of gas pressure on the breakdown voltage. It is noticeable that this equation is only valid for homogeneous fields and usually used for the consideration of metallic cathodes. Nevertheless, it can be used to discuss the general phenomena and dependencies of a discharge process. On its way from cathode to anode, the initial electron collides with gas molecules. For a lower gas pressure, the particle density in the gas is lower leading to a higher distance between the collisions. Therefore, the electron gains more kinetic energy which leads to a decreased breakdown voltage. For a very low pressure, the electron will hit the anode before colliding with a gas molecule. The *Townsend* equation does not include the influence of the temperature on the breakdown voltage [15]. An approach to include the temperature dependence into this

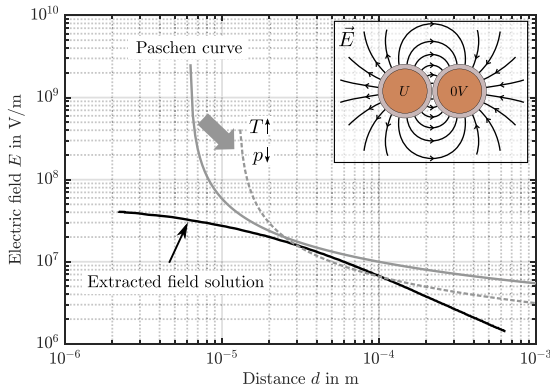


Fig. 3. Influence of temperature and pressure on the electric breakdown field.

equation is the *Dunbar* correction [16]. Following this approach, an equivalent pressure is calculated based on the ideal gas law in the following:

$$p \cdot V = N \cdot k_B \cdot T. \quad (2)$$

This equation states that the number of particles  $N$  decreases with an increasing temperature  $T$  inside an ideal gas with volume  $V$ . The *Boltzmann* constant is indicated as  $k_B$ . This leads to the conclusion that a reduction of air pressure and an increase of temperature produce the same effects. The equivalent pressure  $p_t$  can be calculated using the following:

$$p_t = p \cdot \frac{T_0}{T_t}. \quad (3)$$

The original pressure value  $p$  is multiplied by the relation of the original temperature  $T_0$  and the new temperature  $T_t$ . The effects of a reduction in pressure or an increase in temperature using the *Dunbar* correction is exemplarily shown in Fig. 3. The *Paschen* curve is displayed at normal conditions and at increased temperature or pressure. Additionally, an exemplary solution for the electric field inside the geometry of two adjacent wires is shown. It has to be noted, that only the part of the field lines in air is shown for a better understanding. The field lines start and end at the conductor surfaces. The distance  $d$  relates to the length of the corresponding field lines. The electric field value is the maximum value along the field line. It can be seen in the figure, that the change in temperature and pressure can lead to an intersection with the field solution which means that the electric breakdown field is locally exceeded. Additionally, the variation in temperature also affects the permittivity of the insulation material. It can be seen in [17] that the permittivity of polyester-imide significantly increases when increasing the temperature. Consequently, this leads to an increased electric field between two adjacent wires.

Increased humidity leads to moisture between the wires. Due to the high permittivity of moisture, the electric field can be locally exceeded leading to an increased electric field strength in the air enclosure and thus, a decreasing PDIV. For moisture, a permittivity of 80 can be assumed [18]. Additionally, the moisture influences the material properties of the insulation leading to a changed relative permittivity due to the adsorbed

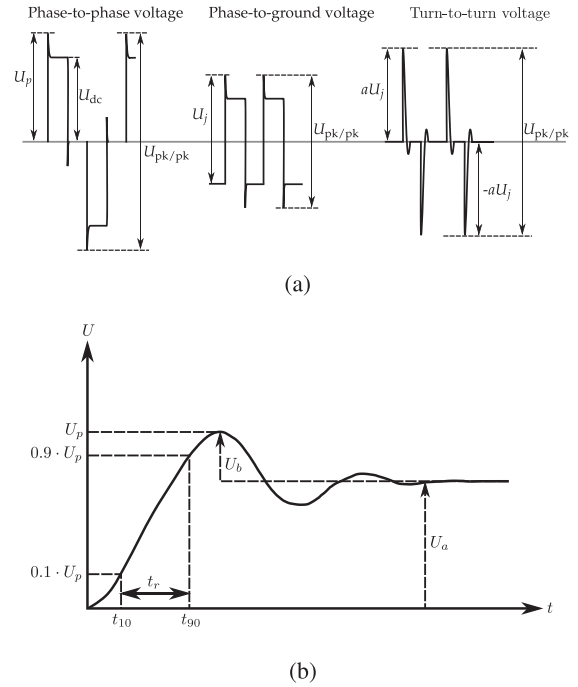


Fig. 4. Voltage pulses stressing the insulation (a) and the definition of a unipolar test pulse (b) according to IEC 60034-18-41 [8].

water molecules. Another reason is the influence of surrounding moisture on the release of initial electrons which incept the PD [14], [19].

Ambient conditions also influence the PDEV. The PDEV is always less than or equal to the PDIV regarding a bipolar voltage waveform. The PDEV mainly depends on the charge carrier accumulation on the insulation surfaces. A higher amount of charge carriers leads to a higher electric field component  $E_{sc}$  which in turn leads to a lower PDEV. This field component is depending on parameters of the voltage waveform like the switching frequency. It can be assumed that the ambient conditions, especially humidity and temperature, influence the attachment and decay process of charge carriers.

### III. CALCULATION OF THE TEST VOLTAGE

In this section, the calculation of the test voltage for the interturn insulation according to IEC 60034-18-41 is explained. The standard provides different enhancement factors depending on the operation conditions, that are multiplied by the dc-link voltage. The result is the test voltage which the insulation system must withstand without the inception of a partial discharge.

#### A. Electrical Stress

The different voltage waveforms stressing the insulation system are pictured in Fig. 4(a). Between two different phases, bipolar voltages occur where the overshoot factor  $OF$  is defined by the relation of the peak voltage  $U_p$  and the final voltage value  $U_a$  [cp. Fig. 4(b)] as indicated in (4). This factor defines

**TABLE I**  
DIFFERENT STRESS CATEGORIES DEPENDING ON THE  
OVERSHOOT FACTOR [8]

Stress category	Overshoot factor (OF)	Impulse rise time $t_r$ in $\mu\text{s}$
A - Benign	$OF \leq 1.1$	0.3
B - Moderate	$1.1 < OF \leq 1.5$	
C - Severe	$1.5 < OF \leq 2.0$	
D - Extreme	$2.0 < OF \leq 2.5$	

the corresponding stress category (see [Table I](#))

$$OF = \frac{U_p}{U_a}. \quad (4)$$

It has to be noted, that [Fig. 4\(a\)](#) displays a simplified version of the actual waveforms. Regarding the turn-to-turn voltage waveform studied in this article, factor  $a$  is used to estimate the maximum voltage stressing the interturn insulation. In reality, it is depending on the switching behavior of the inverter as well as the propagation velocity of the voltage pulses and the wire distribution inside the slot. The latter aspects are not covered by the standard. It has to be noted that the stress categories strongly correlate to the cable length. In inverter-driven electrical machines, usually very short cables are used. However, stress category A with an overshoot factor of 1.1 is very hard to reach, especially when semiconductors with short rise times are used. An overshoot factor of 2 is considered for an electrical machine with long connection cables. The upper limit value of 2.5 relates to extreme conditions in special applications [8].

It is assumed that the interturn insulation is stressed by a part  $a$  of the jump voltage  $U_j$ . The jump voltage  $U_j$  corresponds to the phase-to-phase voltage multiplied by a factor of 0.7 as stated in (5). This factor is empirically determined and is related to the potential shift of the zero point of the converter. The value is linked to the capacitive rise up to 1/3 leading to a factor of about 0,7 [8]

$$U_j = 0.7 \cdot U_p. \quad (5)$$

The factor  $a$  is defined by (6) and indicates the relationship between the applied turn-to-turn voltage  $U$  and the jump voltage  $U_j$

$$a = \frac{U}{U_j}. \quad (6)$$

In [Fig. 5](#), the relation between the rise time of the voltage and the factor  $a$  is given. It can be seen that for a rise time below 50 ns almost the full jump voltage is stressing the interturn insulation. For a rise time below 50 ns, which is expected to be the case for applications with fast-switching semiconductors, the factor  $a$  is not specified.

## B. Temperature

The standard defines a safety factor of 1.3 for the influence of increased temperature concerning the phase-to-phase and the turn-to-turn insulation. This assumption is based on empirical

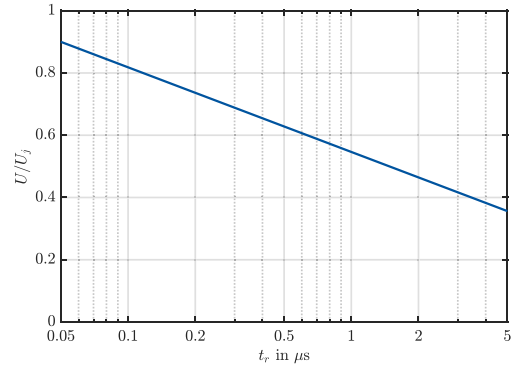


**Fig. 5.** Factor  $a$  in relation to the rise time according to IEC 60034-18-41 [8].

data for the PDIV decrease between 20 °C and 155 °C. However, the applicability is not explicitly limited to a temperature of 155 °C. The effect for the phase-to-ground test is expected to be lower as the effect of cooling is higher. Therefore, the PDIV is decreased by only 5 % to 10 % [8]. This influence is considered in a temperature factor  $TF$ .

## C. Partial Discharge Safety Factor

The utilization of another enhancement factor is based on the fact that the PDEV is lower than the PDIV according to the influence of charge carrier accumulation since the external field is bipolar. As described before, the released charge carriers create an electric field opposite to the external field. The standard states that the PDEV is known to be 25 % lower than the PDIV [8]. This value is empirically determined. If a partial discharge is incepted due to a transient overvoltage, the partial discharge activity has to stop at normal conditions. Otherwise the winding would suffer from electrical aging. The enhancement factor  $PD$  is defined by the following:

$$PD = \frac{PDIV}{PDEV}. \quad (7)$$

## D. Aging

During operation, the insulation system is exposed to different aging mechanisms whereby thermal aging is considered to be the major influence. For type-I insulation systems, it can be assumed that electrical aging can be neglected due to the absence of partial discharges. However, in inverter-driven machines, the switching operation and the associated polarization process lead to dielectric heating. Therefore, high dielectric losses can lead to an early breakdown [20], [21]. Other aging influences can be divided into mechanical and chemical aging. An example for mechanical aging is the abrasion of the insulation if adjacent wires get into contact with each other or the stator iron. Impregnating the insulation system reduces the abrasion and increases the heat dissipation to the stator core. Additionally, slot liners are used to prevent the contact between the wires and the stator. Chemical aging occurs, for example, due to harsh ambient conditions such as a high humidity or contact with aggressive chemicals or dirt [22]. Overall, it can be said that

any aging effect causing a thinning of the insulation leads to a reduction of the PDIV as investigated in [23]. In this standard, only thermal aging is considered resulting in an enhancement factor  $AF$  depending on the thermal class temperature and the service temperature during operation

$$AF = 1.2 \cdot \left( 1 - \frac{\text{Class temperature} - \text{Service temperature}}{\text{Class temperature}} \right). \quad (8)$$

Expecting an operation temperature below the thermal class temperature, the maximum value for  $AF$  cannot exceed 1.2.

### E. Test Voltage

According to the standard, the test voltage for the insulation system of inverter-driven electrical machines is calculated on the basis of the dc-link voltage and the previously discussed enhancement factors. It is assumed that the peak-to-peak voltage is the deciding criterion what coincides with the work discussed in [24] and [25]. In the standard, it is therefore assumed that unipolar and bipolar voltage waveforms can be used equally when providing the same peak-to-peak voltage [8]. This assumption simplifies the partial discharge processes and might not be applicable to any configuration. The peak-to-peak voltage to be applied for examining the interturn insulation is determined by the following equation (according to the standard)

$$U_{\text{test,pk/pk}} = 2 \cdot a \cdot 0.7 \cdot U_{\text{dc}} \cdot OF \cdot NF \cdot PD \cdot AF \cdot TF. \quad (9)$$

The enhancement factor  $NF$  considers an estimated variation of  $\pm 10\%$  of the supply voltage and the battery voltage, respectively. It has to be noted that the aging factor is only applied for type tests. The prescribed test voltage pulse has a rise time  $t_r$  of  $0.3 \mu\text{s}$  with a tolerance of  $\pm 0.2 \mu\text{s}$ . The factor 0.7 is associated with the capacitive shift of the ground potential of the machine relatively to the ground potential of the dc-link.

## IV. MEASUREMENT SETUP

In this section, the measurement setup for the partial discharge measurement is described. To evaluate the influence of the ambient conditions, PDIV and PDEV are measured on twisted pairs representing the interturn insulation of an electrical machine. The setup is schematically sketched in Fig. 6(a). An HVDC source provides a dc-voltage in the range between 0 and 1500 V. The silicon carbide (SiC) module, which is introduced in [26], consists of an H-bridge of CREE C2M0045170D MOSFETS (metal-oxide-semiconductor field-effect transistor) to provide a bipolar impulse voltage. Since the influence of ambient conditions is studied, the specimen is located inside an oven, a climate chamber or a vacuum chamber. The specimen is contacted via cables with a length of 1.5 m. The cable length was determined to be the minimum length needed to contact the specimens inside the oven and climate chamber. The inception of partial discharges is studied by the evaluation of the signal spectrum measured by a high frequency antenna. The type of antenna used in this work is from the 100 Series EMC Probes from Beehive Electronics. The model of the spectrum analyzer

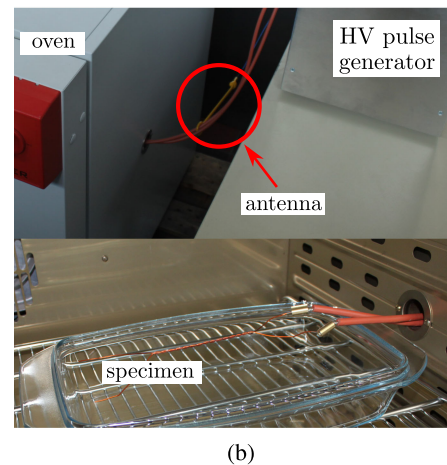
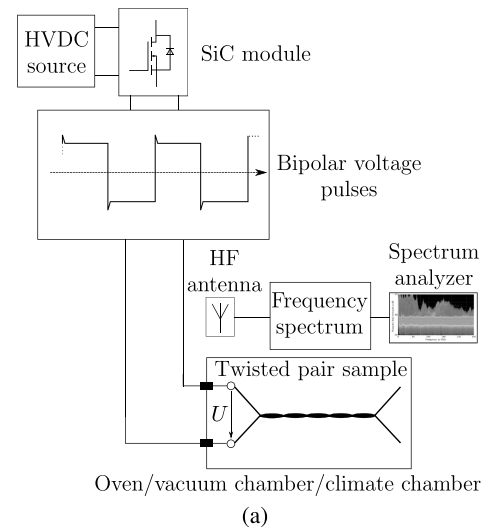


Fig. 6. Measurement setup of the performed partial discharge tests.

used is the Tektronix RSA306B (real-time spectrum analyzer). The measured spectrum is either the magnetic or electric field depending on the antenna used. The average distance between the antenna and the specimens is about 0.5 m. In Fig. 6(b), two sections of the test bench setup are shown. In the top picture, the SiC-module (right side), the UHF-antenna (encircled) and the oven are shown. The antenna used in this setup is sensitive to magnetic fields. One of the connection cables is fed through the loop of the antenna. The specimen (shown in the bottom picture) is placed inside the oven and contacted via cables.

### A. Specimens

To represent the interturn insulation, twisted pair specimens are used for the partial discharge tests. These are qualified to derive the voltage stress level to be applied between two parallel conductors of a motorette or a stator. With regard to the partial discharge tests, equivalent results are expected, but the voltage distribution along the machine winding cannot be reproduced [8]. Therefore, this testing method can be seen as worst-case scenario expecting the full voltage drop between two adjacent windings. The specimens are produced according to IEC 60172-0-1 [27]. The parameters of the studied wire are

TABLE II  
PARAMETERS OF THE WIRE

Parameter	Value
Commercial name	Dahréntråd DAMID 200 [28]
Conductor diameter	1 mm
Insulation grade <sup>1</sup>	Grade 2
Insulation basecoat	THEIC-modified polyester or polyesterimid (PEI)
Insulation overcoat	Polyamide-imide (PAI)
Thermal Class	N
Number of twists	8

<sup>1</sup>according to IEC 60317-0-1

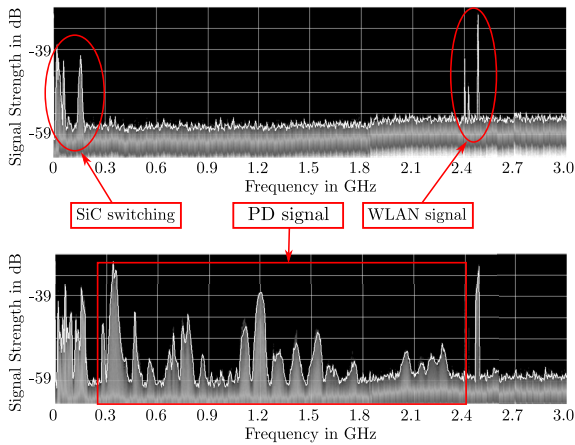


Fig. 7. Frequency spectrum without (above) and with (below) the occurrence of partial discharges.

listed in Table II. For a conductor diameter of 1 mm, according to IEC 60317-0-1 [27], the increase of the outer diameter of the wire due to the insulation has to be in the range of 63 and 94  $\mu\text{m}$  for Grade 2. Based on this specification, the insulation thickness is expected to be in the range of 31.5 and 47  $\mu\text{m}$ .

### B. Partial Discharge Detection

There are numerous different methods to detect partial discharge activity. The appropriate choice is a crucial part and depends on the application. In this article, partial discharge tests are carried out inside an oven, a vacuum chamber and a climate chamber. The utilization of a high frequency antenna provides the best results in comparison to PD detection by measurement of the current at the specimen's terminals. Usually, commercial test systems using an antenna only evaluate a small bandwidth of the frequency spectrum. In this article, the spectrum up to 3 GHz is studied. In Fig. 7, the frequency spectrum with and without presence of partial discharge is shown. It can be seen that partial discharge activity can be characterized over a large bandwidth. In some parts of the frequency range, it is not trivial to separate the PD signals from the signal without PD. These critical parts depend on the location of the antenna and the other properties of the measurement setup. To achieve the best results, the full

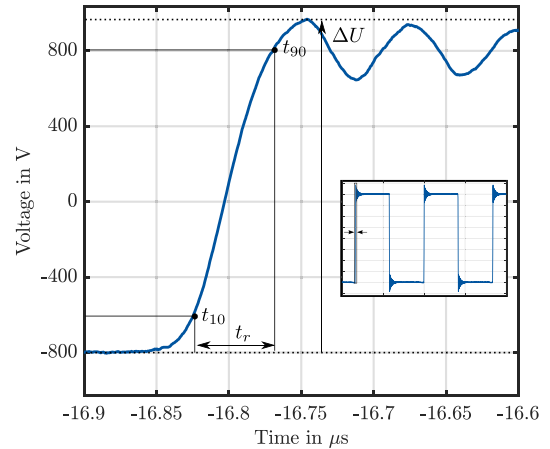


Fig. 8. Bipolar test voltage.

spectrum up to 3 GHz is used for each measurement. The exemplary spectrum shows that the signal without presence of partial discharges is noisy. Particularly in the range between 0 and 200 MHz, the amplitude of the measured signal strength is high which can be explained by the switching operation of the MOSFETs inducing frequencies in this range. The amplitude of this signal is sensitive to the location of the antenna and the shielding of the SiC module. In the range of 2.4 GHz, the signal is noisy due to the Wireless Local Area Network (WLAN) signal. Between these frequency ranges, the PD signal can be clearly separated. When partial discharges occur, a significant change of the signal is instantly visible over a large bandwidth when the partial discharge inception voltage is reached.

### C. Test Voltage

The applied test voltage is exemplarily shown in Fig. 8. The voltage waveform is measured at the terminals of the specimen. In this case, the dc-link voltage is set to 800 V at a rise time  $t_r$  of 80 ns and a switching frequency of 60 kHz. The short rise time causes a peak voltage of 973 V resulting in an overshoot factor of 1.22 and a voltage slew rate of 25 kV/ $\mu\text{s}$ . The switching voltage  $\Delta U$  is 1773 V. According to the standard, any voltage waveform could be used providing the same peak-to-peak voltage. As stated in Section III-E, this specification might not represent real conditions. It is therefore assumed, that a bipolar test voltage with fast rising voltage pulses can best represent the actual electrical stress during inverter operation. Additionally, the PDEV is strongly depending on charge carrier phenomena (cp. Section II-A). The prescribed test voltage pulse by the standard can not represent the fast switching operation of new generation semiconductors since it is known that the rise time of the voltage pulse has a significant effect on the PDIV [29], [30]. During the partial discharge measurement, the voltage was increased or reduced manually by about 2  $\text{Vs}^{-1}$ .

## V. MEASUREMENT RESULTS

In this chapter, the measurement results are discussed. A bipolar test voltage is applied to the specimens. Once a partial

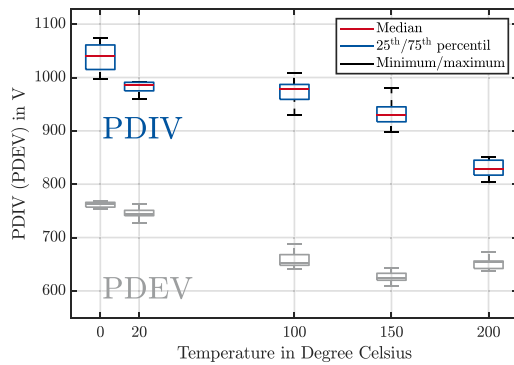


Fig. 9. Dependence of PDIV and PDEV on the temperature.

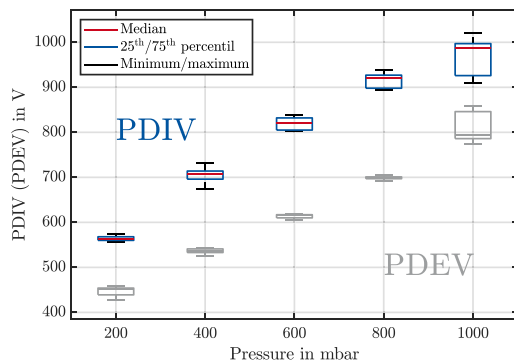


Fig. 10. Dependence of PDIV and PDEV on the air pressure.

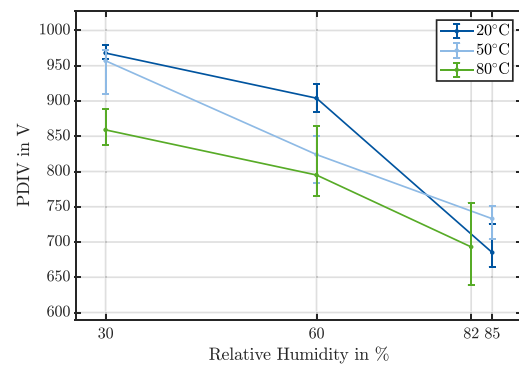
discharge occurs, a PD is incepted at each voltage pulse due to the field enhancement of the charge carrier when the voltage polarity is changed. Therefore, all results relate to the repetitive PDIV and PDEV. The specified voltage values refer to the dc-link voltage value.

### A. Temperature

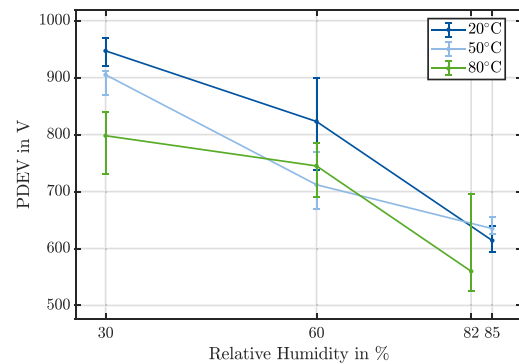
The PDIV and PDEV are measured for different temperatures on ten specimens at uncontrolled humidity. From 0 °C to 20°C, the measurements are performed in the climate chamber as well as for higher temperatures in an oven. The results are shown in Fig. 9. Originating from 20°C, it can be seen that the PDIV increases for a lower temperature and decreases for a higher temperature. From 20°C to 200°C, the mean value of the PDIV decreases from 982 to 829 V corresponding to a relative decrease of 15%. The most significant decrease can be seen between 150°C to 200°C which confirms the preliminary examinations in [15]. The PDEV values follow the course of the values of the PDIV except at 200°C where the PDEV slightly increases.

### B. Air Pressure

The influence of the ambient pressure on the PDIV is measured between 200 and 1000 mbar in equidistant steps on ten specimens. The results are shown in Fig. 10. It can be seen that the ambient pressure significantly influences the measurement results. The mean value of the measured PDIV decreases from



(a)



(b)

Fig. 11. Dependence of PDIV (a) and PDEV (b) on the combined effect of relative humidity and temperature.

972 to 564 V which corresponds to a relative decrease of 42%. The values for the PDEV decrease in the same way as the values for the PDIV.

### C. Humidity

The influence of humidity on the PDIV and PDEV is measured for three different values of the relative humidity at different temperature values on five specimens. At 80°C, the maximum achievable value for the relative humidity is 82%. The results presented in Fig. 11 indicate that the relative humidity significantly affect the PDIV and PDEV. It can be derived that the curves for the different temperatures get closer for higher values of the humidity for the PDIV. The largest drop of the PDIV can be investigated between 60% and 85% relative humidity corresponding to a relative decrease of 24% of the mean value. The results of the measured PDEV follow the course of the PDIV.

### D. PD Safety Factor

The PD safety factor gives the ratio of the PDIV and PDEV. The results for all measurements are depicted in Fig. 12. The vertical axis gives the number of measured values for the corresponding values on the horizontal axis. The range of the value is between 1.02 and 1.57 with a cluster point at around 1.3. It can be seen that the influence of the environmental conditions can be divided into different regions.

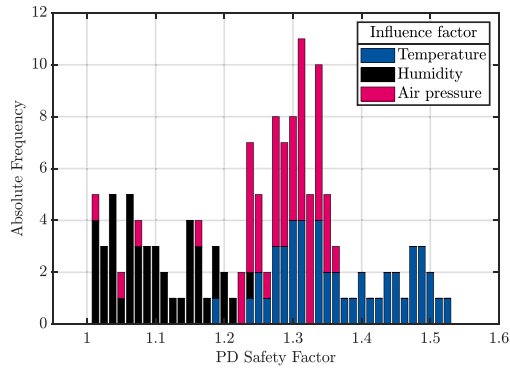


Fig. 12. Absolute frequency of the PD safety factor depending on the different influence factors.

TABLE III  
EXEMPLARY CONDITIONS

Parameter	Value
DC-link voltage	800 V
Voltage rise time	80 ns
Maximum winding temperature	200 °C
Maximum relative humidity	85 %
Estimated maximum altitude	5500 m
Minimum ambient pressure	500 mbar

For the measurements influenced by humidity, the ratio of PDIV and PDEV is between 1.02 and 1.2 with a mean value of 1.09. It can be assumed that the presence of high humidity increases the surface conductivity of the insulation leading to a faster decrease of the amount of charge carriers. The air pressure influence leads to results in a range of 1.02 to 1.37, where most results are between 1.2 and 1.37. The temperature influence causes comparatively high values for the PD safety factor up to 1.57 with a mean value of 1.38. The highest values occur between 100°C and 150°C.

## VI. DISCUSSION

Since the tests are usually performed at room temperature, the ambient conditions must be extrapolated to the expected conditions during operation. This can be realized by applying certain enhancement factors as the standard describes. The measurement results show that all three ambient influence factors significantly affect the partial discharge resistance of the insulation system.

### A. Calculation of the Ambient Enhancement Factor

For an exemplary automotive application, the proposed test voltage is calculated for the conditions listed in Table III. According to Fig. 5, the rise time of 80 ns corresponds to the value of 0.85 for the factor  $a$ . For an 800 V-system, the voltage for qualification tests of the interturn insulation is calculated in (10), taking into account that the dc-link voltage can increase by 10%. Furthermore, a maximum overshoot factor  $OF$  of 1.25 is applied, corresponding to stress category B according

TABLE IV  
CALCULATED ENHANCEMENT FACTORS

Enhancement factor	Worst-case parameter	Value
$TF$	200 °C	1.15
$RH$	85 %	1.24
$PF$	500 mbar	1.25
$PD$	-	1.41

to Table I. The RMS-value of the line voltage is below 700 V which means that a type-I insulation system is considered. The reference point for the studied maximum height in this article is the Khardung Pass in India (above 5 km height), which is considered the world's highest motorized pass.

$$U_{\text{test,pk/pk}} = 2 \cdot 0.85 \cdot 0.7 \cdot 800 \text{ V} \cdot 1.25 \cdot 1.1 \cdot EF_{\text{amb}} \\ = 1309 \text{ V} \cdot EF_{\text{amb}}. \quad (10)$$

It has to be noted that the altitude of 5500 m is regarded to depict the worst case for the operation of an automotive application. Certainly, an altitude of about 3000 m matches the maximum altitude for most electric vehicles. The factor  $EF_{\text{amb}}$  is the proposed enhancement factor which results from the ambient conditions including the safety factor  $PD$ , the temperature enhancement factor  $TF$ , the humidity enhancement factor  $RH$  and the pressure enhancement factor  $PF$ . It has to be noted that the ambient influences cannot be evaluated separately, therefore a simple multiplication of different worst-case factors might not depict the real conditions and thus overestimate the electrical stress. For example, a high humidity and a temperature above 100°C at the same time are not realistic. Hence, the combined effect of temperature and humidity is investigated as done in [31]. For the calculation of the enhancement factor in (11), the maximum of  $RH$  and  $TF$  is calculated to consider the worst-case conditions. It is assumed that the qualification tests of the interturn insulation are usually carried out at a controlled temperature and humidity (20°C and 60% relative humidity). The enhancement factors listed in Table IV are calculated according to the measurement results. Originating from standard conditions (20°C, 60% relative humidity and 1000 mbar), the measurement results from the worst-case conditions are compared resulting in an enhancement factor for the different ambient influence factors. The values for the enhancement factors are calculated from the relation of the measured mean value of the PDIV at normal conditions and the PDIV for the worst-case parameter. The derivation of the safety factors can be seen as an example for the air pressure in Fig. 13.

It is noticeable that in this case, the influence of high humidity is expected to be larger than a high temperature. For the PD safety factor, the right choice is crucial. From the measurement results it is obvious that a value of 1.25 as proposed by the standard could underestimate the electrical stress on the interturn insulation. Assuming that the operating temperature of the winding is higher than 100°C, the ratio of PDIV and PDEV is expected to be between 1.38 and 1.57. In this example, a value of 1.41 is assumed, which corresponds to the mean value of the



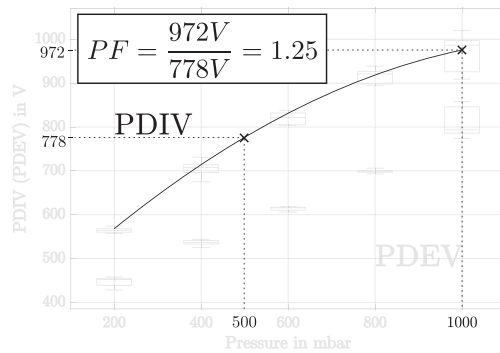


Fig. 13. Calculation of the air pressure enhancement factor.

measured PD safety factor between 100°C and 200°C. Due to the limits of the current laboratory equipment, the air pressure could not be varied at the same time. However, with reference to (1) and (2), it can be assumed that a multiplication with the pressure factor  $PF$  is valid. The ambient enhancement factor is exemplarily calculated as follows:

$$\begin{aligned} EF_{\text{amb}} &= \max(TF, RH) \cdot PF \cdot PD \\ &= 2.19. \end{aligned} \quad (11)$$

The resulting test voltage is calculated as 2867 V. According to the standard, the maximum enhancement factor is 1.63, which is based on the fact that a temperature above 155°C is not considered. The resulting test voltages for qualification tests of the interturn insulation according to the standard is 2134 V. For the example in this article, the proposed test voltage is 34% higher. When comparing these results to the standard, it has to be noted that the superior standard IEC 60034-1 [32] defines the maximum altitude to 1000 m, which means that the standard does not consider the pressure conditions investigated in this work. This fact illustrates that the standard is not without further ado applicable to automotive traction drives.

### B. Interturn Voltage

It can be said that the calculation of the required test voltage is subject to further uncertainties. The factor  $a$  represents the worst-case stress for the interturn insulation depending on the rise time of the voltage pulse. However, using this factor does not provide an accurate estimate for all machines. In a real application, the voltage distribution depends on many factors, e.g., the windings scheme, the inductance of the winding, the wave propagation velocity and others. Furthermore,  $a$  is not specified for a rise time below 50 ns. Future inverters are expected to reach a rise time below this value. Therefore, modeling and measurement of the voltage distribution has great potential to increase the accuracy of the required test voltage. An exemplary measurement setup and a method to model the voltage distribution is shown in [33].

## VII. CONCLUSION

In this article, the calculation of the test voltage for the winding insulation was discussed. The standard IEC 60034-18-41 provided a method based on an enhancement factor for the

temperature and a PD safety factor considering the ratio of PDIV and PDEV. For type tests, an additional aging factor was applied. Ambient influences such as air pressure and humidity were not mentioned in the standard IEC 60034-18-41.

In this work, partial discharge tests were performed on twisted pair samples to study the influence of ambient conditions on the PDIV and PDEV. It was identified that air pressure and humidity had a significant influence and therefore had to be considered during the design and test process of the insulation system. Exemplary ambient conditions for an automotive application studied in this work were not regarded by the standard IEC 60034-18-41. The temperature value was outside the parameters regarded by the standard. The test voltage was consequently calculated based on the performed measurements. It was shown that the calculated voltage is 34% higher than the test voltage prescribed by the standard.

The results showed that the design based on general safety factors, particularly at harsh ambient conditions, could lead to an underestimation of the electrical stress and to an early breakdown of the insulation system. Additionally, it was discussed that a simple multiplication of several enhancement factors might not depict the real stress. In this work, the combined effect of the increase of humidity and temperature on the PDIV and PDEV was studied. Considering that, for example, a high humidity and a temperature above 100°C was not a realistic scenario, the different enhancement factors were evaluated separately. Using the measurement results, it was possible to use the standard method of calculating the test voltage based on safety factors and extend it to operation conditions which are not covered yet.

## REFERENCES

- [1] C. Jung, "Power up with 800-V systems: The benefits of upgrading voltage power for battery-electric passenger vehicles," *IEEE Electr. Mag.*, vol. 5, no. 1, pp. 53–58, Mar. 2017.
- [2] B. Wrzcionko, J. Biela, and J. W. Kolar, "SiC power semiconductors in HEVs: Influence of junction temperature on power density, chip utilization and efficiency," in *Proc. 35th Annu. Conf. IEEE Ind. Electron.*, 2009, pp. 3834–3841.
- [3] D. Fabiani, "Accelerated degradation of AC-motor winding insulation due to voltage waveforms generated by adjustable speed drives," Ph.D. dissertation, Dept. Electr. Eng., Univ. Bologna, Bologna, Italy, 2003.
- [4] B. Florkowska, P. Zydron, and M. Florkowski, "Effects of inverter pulses on the electrical insulation system of motors," in *Proc. IEEE Int. Symp. Ind. Electron.*, 2011, pp. 573–578.
- [5] A. Ruf, J. Paustenbach, D. Franck, and K. Hameyer, "A methodology to identify electrical ageing of winding insulation systems," in *Proc. Int. Elect. Mach. Drives Conf.*, 2017, pp. 1–7.
- [6] M. Kaufhold, G. Borner, M. Eberhardt, and J. Speck, "Failure mechanism of the interturn insulation of low voltage electric machines fed by pulse-controlled inverters," *IEEE Elect. Insul. Mag.*, vol. 12, no. 5, pp. 9–16, Sep./Oct. 1996.
- [7] V. Madonna, P. Giangrande, L. Lusuardi, A. Cavallini, C. Gerada, and M. Galea, "Thermal overload and insulation aging of short duty cycle, aerospace motors," *IEEE Trans. Ind. Electron.*, vol. 67, no. 4, pp. 2618–2629, Apr. 2020.
- [8] *Rotating Elect. Machines - Part 18-41: Partial Discharge Free Elect. Insul. Syst. (Type I) Used in Rotating Elect. Machines Fed From Voltage Converters - Qualification and Quality Control Tests*, IEC Standard 60034-18-41 ed. I, Nov. 2014.
- [9] A. Cavallini, L. Versari, and L. Fornasari, "Feasibility of partial discharge detection in inverter-fed actuators used in aircrafts," in *Proc. Annu. Rep. Conf. Elect. Insul. Dielect. Phenomena*, 2013, pp. 1250–1253.

- [10] L. Lusuardi, A. Rumi, G. Neretti, P. Seri, and A. Cavallini, "Assessing the severity of partial discharges in aerospace applications," in *Proc. IEEE Conf. Elect. Insul. Dielect. Phenomena*, 2019, pp. 267–270.
- [11] R. Rui and I. Cotton, "Impact of low pressure aerospace environment on machine winding insulation," in *Proc. IEEE Int. Symp. Elect. Insul.*, 2010, pp. 1–5.
- [12] E. Sili, J. P. Cambronne, N. Naude, and R. Khazaka, "Polyimide lifetime under partial discharge aging: Effects of temperature, pressure and humidity," *IEEE Trans. Dielect. Elect. Insul.*, vol. 20, no. 2, pp. 435–442, Apr. 2013.
- [13] L. Lusuardi, A. Rumi, and A. Cavallini, "Assessment techniques to ensure reliable electrical insulation for more electric transportation," in *Proc. 45th Annu. Conf. IEEE Ind. Electron. Soc.*, 2019, vol. 1, pp. 7083–7087.
- [14] P. Wang *et al.*, "Influence of ambient humidity on PDIV and endurance of inverter-fed motor insulation," in *Proc. IEEE Elect. Insul. Conf.*, 2019, pp. 201–204.
- [15] F. Pauli, N. Driendl, and K. Hameyer, "Study on temperature dependence of partial discharge in low voltage traction drives," in *Proc. IEEE Workshop Elect. Mach. Des., Control Diagnosis*, 2019, vol. 1, pp. 209–214.
- [16] W. Dunbar and J. W. Seabrook, "High voltage design guide for airborne equipment," Boeing Aerosp. Co., Seattle, WA, USA, Final Rep. AFAPL-TR-76-41, 1976.
- [17] L. Fetouhi, J. Martinez-Vega, and B. Petitgas, "Electric conductivity, aging and chemical degradation of polyesterimide resins used in the impregnation of rotating machines," *IEEE Trans. Dielect. Elect. Insul.*, vol. 25, no. 1, pp. 294–305, Feb. 2018.
- [18] T. Wakimoto, H. Kojima, and N. Hayakawa, "Measurement and evaluation of partial discharge inception voltage for enameled rectangular wires under AC voltage," *IEEE Trans. Dielect. Elect. Insul.*, vol. 23, no. 6, pp. 3566–3574, Dec. 2016.
- [19] Y. Kikuchi *et al.*, "Effects of ambient humidity and temperature on partial discharge characteristics of conventional and nanocomposite enameled magnet wires," *IEEE Trans. Dielect. Elect. Insul.*, vol. 15, no. 6, pp. 1617–1625, Dec. 2008.
- [20] B. Sonnerud, T. Bengtsson, J. Blennow, and S. M. Gubanski, "Dielectric heating in insulating materials subjected to voltage waveforms with high harmonic content," *IEEE Trans. Dielect. Elect. Insul.*, vol. 16, no. 4, pp. 926–933, Aug. 2009.
- [21] D. Fabiani, G. C. Montanari, and A. Contin, "Aging acceleration of insulating materials for electrical machine windings supplied by PWM in the presence and in the absence of partial discharges," in *Proc. IEEE 7th Int. Conf. Solid Dielect. (Cat. No.01CH37117)*, 2001, pp. 283–286.
- [22] G. Stone, I. Culbert, E. Boulter, and H. Dhirani, *Elect. Insulation for Rotating Machines: Design, Evaluation, Aging, Testing, and Repair (IEEE Press Series on Power Engineering)*. Hoboken, NJ, USA: Wiley, 2014.
- [23] V. Madonna, P. Giangrande, G. Migliazza, G. Buticchi, and M. Galea, "A time-saving approach for the thermal lifetime evaluation of low-voltage electrical machines," *IEEE Trans. Ind. Electron.*, vol. 67, no. 11, pp. 9195–9205, Nov. 2020.
- [24] D. Fabiani, G. C. Montanari, A. Cavallini, and G. Mazzanti, "Relation between space charge accumulation and partial discharge activity in enameled wires under PWM-like voltage waveforms," *IEEE Trans. Dielect. Elect. Insul.*, vol. 11, no. 3, pp. 393–405, Jun. 2004.
- [25] M. Kaufhold, H. Aninger, M. Berth, J. Speck, and M. Eberhardt, "Elect. stress and failure mechanism of the winding insulation in PWM-inverter-fed low-voltage induction motors," *IEEE Trans. Ind. Electron.*, vol. 47, no. 2, pp. 396–402, Apr. 2000.
- [26] K. Hameyer, A. Ruf, and F. Pauli, "Influence of fast switching semiconductors on the winding insulation system of electrical machines," in *Proc. Int. Power Electron. Conf.*, 2018, pp. 740–745.
- [27] *Specifications for Particular Types of Winding Wires - Part 0-1: Gen. Requirements - Enameled Round Copper Wire*, IEC Standard 60 317–0-1, 2013.
- [28] LWW Group, *Product Inf. DAMID 200*. Accessed: Apr. 27, 2021. [Online]. Available: <http://www.lww.se/wp-content/uploads/2014/06/DAMID-200.pdf>
- [29] P. Wang, H. Xu, J. P. Wang, W. Zhou, and A. Cavallini, "The influence of repetitive square wave voltage rise time on partial discharge inception voltage," in *Proc. IEEE Conf. Elect. Insul. Dielect. Phenomena*, 2016, pp. 759–762.
- [30] N. Driendl, F. Pauli, and K. Hameyer, "Modeling of partial discharge processes in winding insulation of low-voltage electrical machines supplied by high  $du/dt$  inverters," in *Proc. 45th Annu. Conf. IEEE Ind. Electron. Soc.*, 2019, vol. 1, pp. 7102–7107.
- [31] T. Kaji, H. Asai, H. Kojima, and N. Hayakawa, "Combined effect of temperature and humidity of magnet-wires on partial discharge inception voltage under inverter-surge voltage," in *Proc. IEEE Conf. Elect. Insul. Dielect. Phenomena*, 2018, pp. 554–557.
- [32] *Rotating Elect. Machines - Part 1: Rating and Performance*, IEC Standard 600 34–1, 2017.
- [33] A. Krings, G. Paulsson, F. Sahlén, and B. Holmgren, "Experimental investigation of the voltage distribution in form wound windings of large AC machines due to fast transients," in *Proc. 22nd Int. Conf. Elect. Mach.*, 2016, pp. 1700–1706.



**Niklas Driendl** received the M.Sc. degree in electrical engineering from RWTH Aachen University, Aachen, Germany, in October 2018.

He started working as a Research Associate with the Institute of Electrical Machines, RWTH Aachen University, in January 2019. His research interests include characterization of insulation systems of electrical machines and modeling of partial discharge processes.



**Florian Pauli** received the M.Sc. degree in electrical engineering from RWTH Aachen University, Aachen, Germany, in April 2017.

He has been working as a Research Associate with the Institute of Electrical Machines, RWTH Aachen University, since May 2017. His research interests include iron loss computations, thermal behavior, overload capability, lifetime models, and the characterization of insulation systems of electrical machines.



**Kay Hameyer (Senior Member, IEEE)** received the M.Sc. degree in electrical engineering from the University of Hannover, Hanover, Germany, in 1986 and the Ph.D. degree in 1992 from the University of Technology Berlin, Berlin, Germany, for working on permanent magnet excited machines.

After his university studies, he worked with the Robert Bosch GmbH, Stuttgart, Germany, as a Design Engineer for permanent magnet servo motors. From 1988 to 1993, he was a Member of staff with the University of Technology Berlin. From 1996 to 2004, he was then a Full Professor of Numerical Field Computations and Electrical Machines with Katholieke Universiteit Leuven (KU Leuven), Leuven, Belgium. Since 2004, he has been a Full Professor and the Director of the Institute of Electrical Machines (IEM), RWTH Aachen University, Aachen, Germany. The characterization and modeling of hard- and soft-magnetic materials is another focus of his work. He has authored/coauthored more than 350 journal publications, more than 700 international conference publications and four books. His research interest focuses on all aspects of the design, control and manufacturing of electrical machines and the associated numerical simulation. His research interests include numerical field computation and optimization, the design and control of electrical machines, in particular, permanent-magnet excited machines, induction machines.

Dr. Hameyer is a Member of the German VDE and a Fellow of the Institution of Engineering and Technology, U.K.